Environmental Technology & Innovation 35 (2024) 103650

Contents lists available at ScienceDirect

Environmental Technology & Innovation

journal homepage: www.elsevier.com/locate/eti

Effects of cellulose nanofibers on soil water retention and aggregate stability

An Thuy Ngo [a,b], Yasushi Mori [a,*], Long Thanh Bui [a]

[a] Graduate School of Environmental and Life Science, Okayama University, Okayama 700-8530, Japan
[b] An Giang University – Vietnam National University, Hochiminh City, Angiang, Viet Nam

ARTICLE INFO

Keywords:
Soil amendments
water-saving polymers
soil moisture improvement
mean weight diameter
irrigation water

ABSTRACT

Innovative solutions that address global challenges such as water scarcity and soil erosion are critical for maintaining sustainable agriculture. Due to their water-absorbing and soil-binding properties, cellulose nanofibers (CNF) can be applied to soil to enhance soil water retention and aggregate stability. In this study, we analyzed the effects of the drying temperature, dosage, irrigation water quality, and soil type on the efficacy of CNFs. Our results revealed that CNF dried at 5°C is more effective at absorbing water than others, and adding 1% CNF enhanced soil water content up to 98%. The CNF samples absorbed water due to their hydrophilic molecular groups and morphological structure, as confirmed by Fourier-transform infrared spectroscopy and scanning electron microscopy. CNF addition increased the soil volumetric water content and prolonged water retention by 22 days in the paddy soil samples, highlighting its potential for drought-prone areas. Furthermore, irrigation water quality, such as pH and cation values, influenced the interactions between CNF and water molecules, suggesting adjustments to the water retention curve. In its hydrated state, CNF promotes colloid flocculation and binds to soil particles, thereby strengthening the bonds crucial for aggregate formation and stability. CNF enhanced macro-aggregate formation by up to 48% and 59% in the masa and paddy soil samples, respectively. Our study emphasizes the potential of CNF for water conservation, soil health, and overall agricultural sustainability.

1. Introduction

Climate change, anthropogenic activities, and other environmental factors threaten global agricultural sustainability by aggravating water scarcity and soil erosion (Alsulaili et al., 2022; Ide et al., 2019; Shao et al., 2023a). Soil water availability and aggregate stability are crucial factors affecting crop productivity by facilitating hydration, nutrient access, and overall soil health (Kang et al., 2022; Mori et al., 2013, 2014; Qi et al., 2022). Soil aggregate stability is among the main physical indicators for plant health as it affects soil aeration, root growth, water holding, erosion, nutrient cycling, and microbial habitat (Jat et al., 2023). Intensifying droughts, stronger typhoons, and increasing non-agricultural water usage further deplete the limited water resources (Gharib et al., 2023; Shao

Abbreviations: CNF, cellulose nanofibers; MS, masa soil; PS, paddy soil; 5DC, CNF dried at 5 °C; 25DC, CNF dried at 25 °C; 45DC, CNF dried at 45 °C; DW, distilled water; TW, tap water; MW, masa soil–extracted water; PW, paddy soil–extracted water; MWD, mean weight diameter; SWRC, soil water retention curve; SA, soil aggregate; SOM, soil organic matter; OM, organic matter.

* Correspondence to: Graduate School of Environmental and Life Science, Okayama University, 3-1-1 Tsushimanaka, Okayama 700-8530, Japan.
E-mail address: yasushim@cc.okayama-u.ac.jp (Y. Mori).

https://doi.org/10.1016/j.eti.2024.103650
Received 28 November 2023; Received in revised form 24 April 2024; Accepted 27 April 2024
Available online 30 April 2024

et al., 2023a). Moreover, these factors weaken soil integrity, leading to soil cracking and exacerbated erosion (Morioka et al., 2023; Quintana et al., 2023). Thus, addressing these challenges is critical for ensuring water availability and global food security (Shao et al., 2023a).

Novel soil amendments, such as water-absorbing polymers, offer innovative solutions to agricultural challenges (Dhiman et al., 2021; Marczak et al., 2022; Situ et al., 2023; Zhang et al., 2023). Cellulose nanofibers (CNF), derived from plant biomass, have notable nanoscale dimensions, large surface areas, and hydrophilic properties (Zhang et al., 2023). Apart from enhancing soil water retention and minimizing evaporation (Barajas-Ledesma et al., 2022), CNF may strengthen soil aggregate (SA) stability and improve soil structure, making them highly valuable in water-stressed regions. Due to their multiple advantages, including excellent water storage, and the ability to bind soil particles together along with renewability, biodegradability, and environmental compatibility (Barajas-Ledesma et al., 2022; Bhattacharyya et al., 2021; Reshmy et al., 2021; Shao et al., 2023a; Zhang et al., 2023), CNF, specifically TEMPO-CNF (TEMPO stands for 2,2,6,6-Tetramethylpiperidine-1-oxyl), has received increasing attention.

TEMPO-CNF is produced by specific hydrolysis and oxidation techniques (Kaffashsaie et al., 2021; Djafari Petroudy et al., 2018), and is typically stored in aqueous form due to its inherent hydrophilicity (Šebenik et al., 2020). Changes in the drying process during synthesis can modify CNF structure (Klemm et al., 2018; Stanisławska et al., 2020), affecting soil water retention performance (Andree et al., 2021). However, research on the specific effects of different CNF drying methods on soil moisture conservation in agriculture is limited. Thus, further studies are required to maximize the potential of CNF in improving the water retention capacity of cultivated soils.

Irrigation water quality and soil texture affect the hydraulic characteristics of CNF-amended soils (Bauli et al., 2021; Qin et al., 2022; Zhang et al., 2023). Water quality aspects, such as alkalinity and water cations can alter CNF absorption and swelling behaviors (Chang et al., 2011; Liu et al., 2014). Moreover, soil properties primarily dictate soil's hydraulic conductivity and moisture retention (Bui et al., 2022; Dexter, 2004; Mori et al., 1999). Soil texture and organic content are critical for water retention (Qin et al., 2022; Saha et al., 2020). CNF must be fine-tuned to suit specific soil types (Barajas-Ledesma et al., 2022; Bauli et al., 2021). Therefore, analyzing the effect of CNFs on water retention in various irrigation scenarios and soil types is crucial to optimize its agricultural application.

Hydrocarbon compounds, such as cellulose, starch, and glucose, contribute to soil organic matter (SOM) content (Chavez-Rico et al., 2023; Chen et al., 2023; Mizuta et al., 2015). SOM binds to soil particles through cohesive forces, facilitating SA formation. Upon hydration, these compounds enhance colloid flocculation and adhere to soil particle surfaces, thereby strengthening the chemical bonds involved in SA formation (Abiven et al., 2009; Shao et al., 2023a; Situ et al., 2022). Although CNF is hypothesized to augment SA, its specific mechanisms and effectiveness can differ due to soil texture, organic content, and other properties across soil types. This variability contributes to a limited understanding of the intricate relationship between CNF and SA formation, potentially restricting its perceived utility as a soil enhancer. Thus, it is essential to investigate the effects of CNF on SA formation and stability in various soil contexts.

The aim of this study was to assess the improvement of soil water retention and aggregate stability by CNF produced at various drying temperatures. The specific objectives of this study were to (i) determine the effect of CNF drying methods on the water absorption capacity, (ii) examine the influence of irrigation water quality on soil water retention, and (iii) analyze the relationship between CNF dosage and soil type with respect to aggregate stability. Laboratory tests were performed using three CNF drying methods (cool-, air-, and oven-dried CNF), four CNF dosages (0%, 0.1%, 0.5%, and 1.0%), four irrigation water qualities (distilled, tap, masa soil–extracted, and paddy soil–extracted water), and two soil varieties (sandy and silt loam soils). Our findings offer an effective strategy for increasing water availability, enhancing soil stability, and positioning CNFs as viable soil enhancers.

2. Materials and methods

2.1. CNF, soil, and water

The CNF, a commercially hydrated product from Cellulose Lab (Quebec, Canada), was designated as TEMPO-CNF. Its characteristics, including the unique three-dimensional network structure that significantly contributes to its high water retention and absorption capabilities, are summarized in Table A.1. Initially hydrated CNF was dried at three temperatures: 5, 25, and 45 °C, resulting in different dried-CNF products labeled 5DC, 25DC, and 45DC, respectively. Drying at 5 °C was carried out in a refrigerator with a relative humidity of approximately 20%, at 25 °C in an indoor laboratory environment, and at 45 °C in an oven. The samples were monitored until their moisture content decreased to approximately 10%. Subsequently, the samples were stored in glass bottles with lids for further use.

Two soil samples with different textures suitable for plant growth—sandy or masa soil (MS) and silt loam or paddy soil (PS)—were collected from the cultivated layer (0–200 mm) of two sites in Okayama, Japan: 34° 41'26.0" N, 133° 55'33.5" E for the MS samples and 34° 41'08.3" N, 133° 54'48.9" E for the PS samples. The samples were air-dried and sieved through a 2-mm mesh. The basic properties of these soils are listed in Table A.2. Particle size distribution was determined using a laser diffraction analyzer (SALD-3100; Shimadzu, Kyoto, Japan). Porosity was calculated from the particle and bulk densities (Dane et al., 2002). Organic matter (OM) was quantified using the loss-on-ignition method (Sparks et al., 1996). A soil sample of 10 g was heated at 450°C for 4 hours to ensure accurate OM estimation.

Four types of water were used in this study: distilled water (DW), tap water (TW), masa soil–extracted water (MW), and paddy soil–extracted water (PW). The extraction procedure was adapted from a previously reported saturated extraction method (Sparks et al., 1996). The pH was determined using a pH meter (Laqua Twin pH-11B; Horiba, Kyoto, Japan). Cations were analyzed using simultaneous ICP atomic emission spectrometry (ICPE-9820; Shimadzu, Kyoto, Japan). The important quality parameters of water

used are in Table A.3

2.2. Water absorption

The effect of the drying method on the absorbency of CNF was investigated. MS was selected because of its limited OM content, which minimizes the nutrient influence. Three dried CNF samples (5DC, 25DC, and 45DC) were mixed separately with MS at a 1% CNF ratio. Dried CNF and bare soil samples were used as the controls. The samples were placed in 15-mL polypropylene tubes; a 1-mm hole at the bottom was covered with a cotton pad to prevent soil drainage. The tubes were submerged in DW for 1, 5, 15, 30, and 60 min, followed by 60-min increments in 480 min. After each immersion, the samples were weighed to determine absorption capacities. The absorption capacity was calculated using Eq. (1), where W_t (g) and W_o (g) are the weights of the swollen and dried samples, respectively (El Idrissi et al., 2022).

$$Absorption\ capacity\left(g.g^{-1}\right) = \frac{W_t - W_o}{W_o} \tag{1}$$

2.3. Repeated water absorption

After the initial water absorption experiment, the samples were used for repeated absorption investigations. Each sample was saturated in DW for 24 h and dehydrated in an oven at 32 °C. The samples were subjected to five wet-dry cycles, alternating between immersion in DW and oven drying. The repeated absorption capacity in each cycle was measured using Eq. (1).

2.4. Soil water retention curve

The effect of different irrigation water qualities on the soil water retention curve (SWRC) in CNF-amended soil was assessed using four types of water to cover a broad range of scenarios. DW and TW represented the cleanest irrigation scenarios, while MW and PW simulated degraded water conditions. This selection strategically encompassed the spectrum of potential irrigation water qualities, from ideal to highly challenged conditions.

The SWRC of the CNF-amended soil samples was evaluated using the centrifuge outflow method (Bui and Mori, 2021), illustrating the relationship between soil suction and water content. Initially, 1% 5DC was mixed with 15 g of MS and placed in tubes as described in Section 2.2. These tubes were then immersed separately in each water type. After saturation, the samples were centrifuged at 100, 300, 500, 800, 1000, and 1500 rpm for 30 min, corresponding to 13, 121, 337, 862, 1346, and 3029 kPa, respectively. Subsequently, they were oven-dried at 105 °C for 24 h. The volumetric water content was calculated using Eq. (2) (Campbell and Campbell, 2013), where m_w is the mass of water retention after centrifugation, m_d is the mass of oven-dry soil, ρ_d represents soil bulk density, and ρ_w represents water density (typically, $\rho_w = 1$ g.cm^{-3}).

$$Volumetric\ water\ content\left(cm^3.cm^{-3}\right) = \frac{m_w}{m_d} \times \frac{\rho_d}{\rho_w} \tag{2}$$

2.5. Soil water retention time

The interactive effects of CNF application rates and soil types on soil water retention were analyzed. Two soil types (MS and PS) and four 5DC dosages (0%, 0.1%, 0.5%, and 1.0%) were used. The soil samples were combined with the specified CNF dosages and placed in prepared tubes. Subsequently, the tubes were immersed in DW for full saturation before weighing. The tubes were then transferred to an incubator (CN-40A; Mitsubishi, Tokyo, Japan) at 32 °C. This temperature was selected to simulate the average daytime temperatures common in many agricultural countries, which is pertinent for evaluating the potential real-world application of CNF in agricultural fields. Daily water retention was measured until reaching a constant weight. The water retention ratio was calculated using Eq. (3), where W_e (g) represents the mass of the control sample at complete equilibrium (Day 0), and W_t (g) is the mass of the treatment samples on Day t (Barajas-Ledesma et al., 2022).

$$Water\ retention\ ratio(WR)\quad (\%) = \frac{W_t}{W_e} \times 100 \tag{3}$$

2.6. Soil aggregate stability

SA stability is pivotal for evaluating soil health and its susceptibility to erosion and degradation processes. It reflects the erosion resistance capacity, water infiltration rate, nutrient cycling, and plant root penetration. Enhanced SA stability is crucial for promoting sustainable agricultural practices and environmental conservation. Therefore, this study aims to highlight the role of CNF in enhancing SA stability, which contributes to maintaining soil health and enhancing crop productivity.

A setup was prepared to analyze SA stability, reflecting the experimental conditions of soil water retention tests. Specifically, 500 g of MS and PS was each mixed with four 5DC dosages (0%, 0.1%, 0.5%, and 1.0%) and placed in the incubator after saturation. Samples were collected on Days 0, 5, 10, 15, 25, and 45 over the 45-day observation period to determine SA size distribution.

The SA stability was assessed using the mean weight diameter (MWD) index following the wet sieving method (Elliott, 1986). For

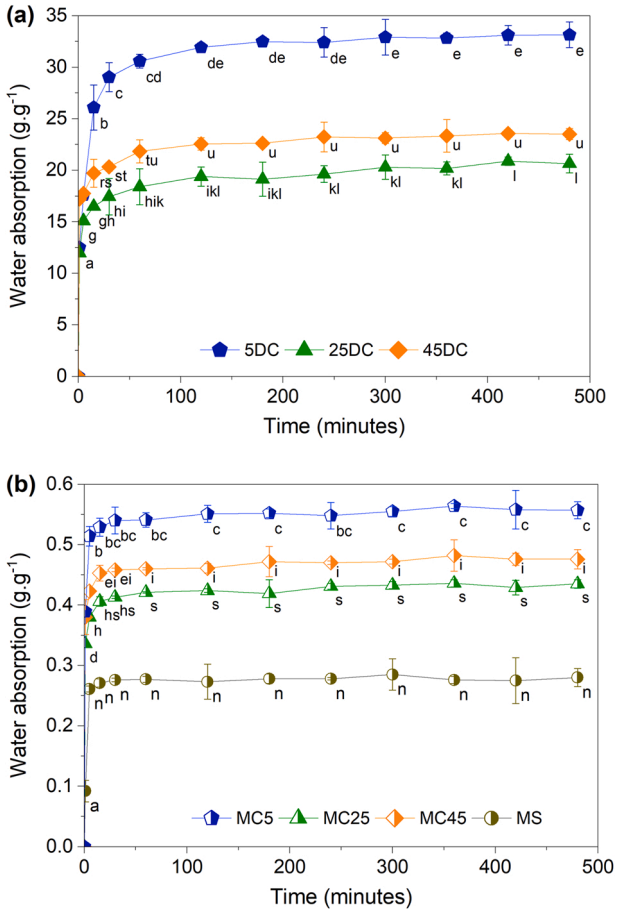

Fig. 1. Water absorption of dried CNF (1a) and CNF-amended soil (1b). Masa soil combined with 1% 5DC (MC5), 25DC (MC25), and 45DC (MC45). CNF, cellulose nanofibers; MS, masa soil; 5DC, 25DC, and 45DC, CNF dried at 5, 25, and 45 °C, respectively.

this assessment, soil samples weighing 5 g each were subjected to wet sieving using sieves with mesh sizes of 53, 250, 850, and 2000 micrometers. The MWD was calculated using Eq. (4), where X_i is the mean diameter of aggregates of each particle size (mm), W_i is the proportion of aggregates of the corresponding particle size in the total sample, and n is the number of aggregate particle sizes (Situ et al., 2022).

$$\text{Mean weight diameter}(MWD) = \sum_{i=1}^{n} X_i.W_i \quad (4)$$

2.7. FTIR and SEM analysis

Dried CNFs were analyzed by a Fourier-transform infrared (FTIR) spectrophotometer equipped with an attenuated total reflection (ATR) (Cary630; Agilent Technologies, Santa Clara, CA, USA). Spectra were obtained from 4000 to 650 cm^{-1} at a resolution of 4 cm^{-1}. The surface morphology of the cellulose fibrils was assessed by scanning electron microscopy (SEM) (JSM-6010LA; JEOL, Tokyo, Japan) in the vacuum mode.

2.8. Data analysis

OriginPro 2023 was used for data processing and graphical representation. Experimental data are presented as mean values from three replicates (n = 3). Two-way analysis of variance (ANOVA), followed by pairwise comparisons and Tukey's HSD post-hoc test, was performed using SPSS 25.0 (IBM Corporation, Armonk, NY, USA).

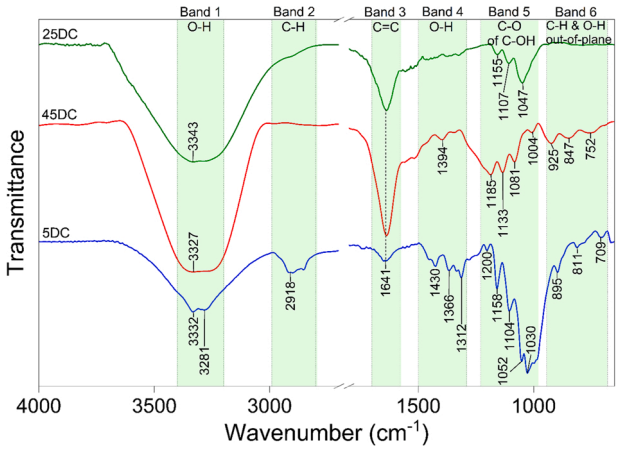

Fig. 2. ATR-FTIR spectra of three dried CNFs. CNF, cellulose nanofibers; 5DC, 25DC, and 45DC, CNF dried at 5, 25, and 45 °C, respectively.

3. Results and discussion

3.1. Effect of CNF drying temperatures on the water absorption behavior

3.1.1. Water absorption

The effect of the CNF drying temperature on its water absorbency is shown in Fig. 1. All the samples showed a similar absorption trend: rapid initial water absorption, followed by a gradual increase until equilibrium. The amended soil samples achieved equilibrium in water absorption faster than the free CNF samples, consistent with the bare soil pattern. There was no significant difference ($p > 0.05$) in the water absorption rate within each type of modified and bare soil samples after 15 minutes, or within each category of the free CNFs after 60 min.

Fig. 1a illustrates the water absorption of the three dried CNF samples. The 5DC sample exhibited the highest absorption of 33.15 ($g.g^{-1}$), expanding 33-fold compared with its dried weight. The water absorption of the three dried CNF samples significantly differed ($p < 0.05$) and is ranked as 5DC > 45DC > 25DC. Fig. 1b depicts a similar trend in the amended soil samples; the 5DC-amended masa soil (MC5) displayed the highest water absorption of 0.56 ($g.g^{-1}$), representing a 98% increase compared with the control (MS). The 45DC-amended (MC45) and 25DC-amended masa soil samples (MC25) exhibited 69% and 55% improvements, with water absorption of 0.47 and 0.43 ($g.g^{-1}$), respectively. Despite the variations in CNF absorption due to drying temperatures, the modified soil samples demonstrated at least a 1.55-fold increase in water absorption compared with the control, suggesting the potential of CNF in soil drought management.

FTIR spectral analysis revealed how the drying temperatures affect CNF chemical structure and water absorption. Fig. 2 illustrates the significant CNF spectral changes upon drying, identifying five distinct groups labeled as bands 1–5. First, drying shifted transmittance and position within the 3400–3200 cm^{-1} region (Fig. 2, band 1), such as 3332 and 3281 cm^{-1} for 5DC; 3327 cm^{-1} for 45DC; and 3343 cm^{-1} for 25DC, corresponding to hydrogen-bonded OH stretching vibrations (Shao et al., 2023b; Wang et al., 2015). As the drying temperature increased, the peak at 3281 cm^{-1} disappeared in the 25DC and 45DC, indicating the reduction in intramolecular hydrogen bonds. Consequently, this phenomenon released free OH groups (Stanisławska et al., 2020), thus explaining the lower water absorbency in the 25DC and 45DC samples than the 5DC sample.

Second, the range of 1500–1290 cm^{-1} (Fig. 2, band 4) displayed a rise in peak intensity within 5DC, aligning with the variation in drying temperature. Multiple peaks in 5DC at 1430, 1366, and 1312 cm^{-1} attributed to the hydrophilic hydroxyl group (Coates, 2006; Stanisławska et al., 2020), reaffirmed the superior water absorption of 5DC compared with the other types. Interestingly, 45DC, subjected to a higher drying temperature than 25DC, retained its peak at 1394 cm^{-1}, whereas 25DC showed no peaks in this range. The disappearance of these peaks indicated reduced hydroxyl groups, leading to the limited water absorption of 25DC compared with that of 45DC. However, these observations contradicted the overall trend, wherein the higher CNF drying temperature reduced the absorption capacity. The drying time discrepancy, with the 25DC sample requiring 12 days compared to only 4 days for both the 5DC and 45DC samples, may suggest changes in its chemical structure or three-dimensional spatial arrangement. This observation serves as a preliminary hypothesis, encouraging further detailed analysis of the CNF structure.

Third, within the spectral range of 1200–1000 cm^{-1}, the identified peaks indicated alcohol groups, specifically the C-O group inherent in alcohols. These peaks corresponded to primary, secondary, and tertiary alcohols (Coates, 2006; Stanisławska et al., 2020), with hydrophilic functionalities (Fig. 2, band 5). The number and intensity of the peaks in this region, ranked as 5DC > 45DC > 25DC, demonstrate the difference in the water absorption of the three dried CNF types.

Fig. 2 (bands 2, 3, and 6) shows the bending of C=C, C-H, and O-H out-of-plane vibrations. The C=C and C-H groups are indicative of the presence of hydrophobic alkene and alkane groups, respectively, whereas the O-H out-of-plane vibration signals the presence of hydrophilic groups (Coates, 2006; Gill and Wadsö, 1976; Stanisławska et al., 2020). The alkene group (band 3) was observed in all three dried CNF samples. Interestingly, the 5DC sample showed an additional hydrophobic group (band 2 and 6), which typically

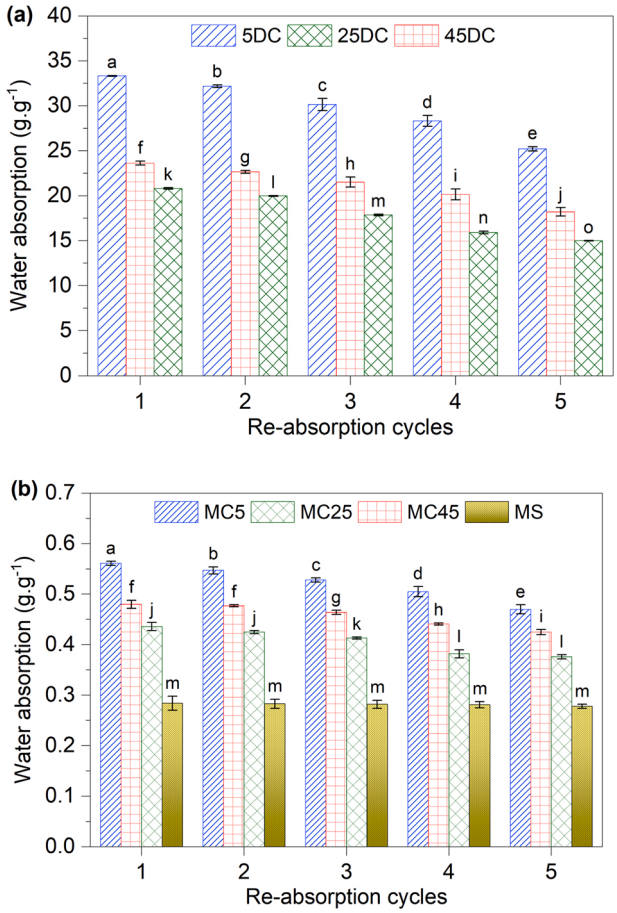

Fig. 3. Water reabsorption of dried CNF (3a) and CNF-amended soil (3b) with five wet/dry cycles. Masa soil combined with 1% 5DC (MC5), 25DC (MC25), and 45DC (MC45). CNF, cellulose nanofibers; MS, masa soil; 5DC, 25DC, and 45DC, CNF dried at 5, 25, and 45 °C, respectively.

reduces water affinity. However, the 5DC sample demonstrated enhanced water absorption. This paradox can be explained by the presence of hydrophilic groups in bands 1, 4, and 5, representing O-H and C-O bonds of C-OH groups, respectively, as previously mentioned. A greater number of peaks linked to hydrophilic groups suggest higher water absorption potential within the CNF structure even in the presence of hydrophobic groups.

These findings may serve as the basis for refining CNF preparation to enhance soil water management. Manipulating the CNF drying temperature could fine-tune its water retention characteristics, thereby promoting CNF formulations with superior water-holding capacities. Such advancements offer a promising approach for innovative soil amendments to mitigate irrigation water scarcity. However, the cost-effectiveness of employing CNF is a critical factor for practical application. A comprehensive assessment of economic viability, including production costs and application at the field scale, is essential to fully realize CNF's potential in agriculture.

3.1.2. Water reabsorption capacity

The re-absorption capacity of CNF during wet-dry cycles, which is critical for soil application reusability, gradually decreased by 22–27% over five cycles (Fig. 3a). Specifically, the water absorption capacity of the 5DC sample decreased by 24% from 33.34 to 25.22 ($g.g^{-1}$) while that of the 45DC and 25DC samples decreased by 22% and 27%, respectively, after five cycles.

The water absorption capacity of the CNF-amended soil samples, labeled MC5, MC25, and MC45, demonstrated a slight decrease over time. Specifically, the reductions in water absorption capacity were quantified at 16% for MC5, 14% for MC25, and 12% for MC45, respectively (Fig. 3b).

The sole analysis of CNF's chemical structure provides an incomplete explanation for the behavior observed in the 25DC sample, underscoring the need for additional investigative methods. Consequently, SEM analysis was employed to delve deeper into the 25DC phenomenon, exploring the relationship between CNF morphology, the multi-cycle drying process, and moisture absorption capacity.

SEM images of the 5DC, 25DC, and 45DC samples at the beginning of the multi-cycle process (Fig. 4a, b, and c) reveal visible variations. The 5DC sample exhibited a delicate, loose, and porous structure, which may indicate a slightly larger pore volume or surface area compared to the initial structure of the other CNF samples. Despite drying at a lower temperature, the 25DC sample

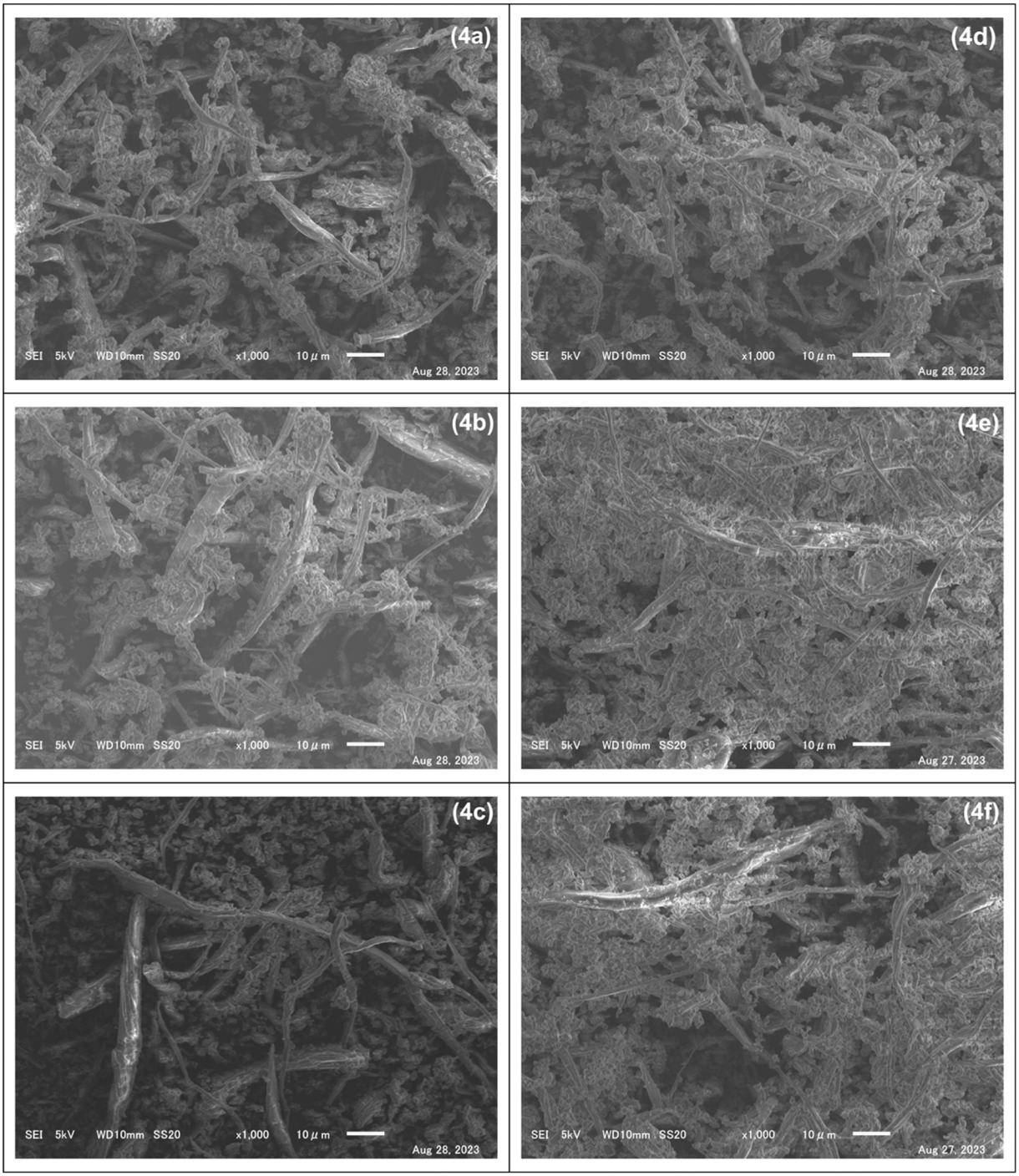

Fig. 4. Scanning electron microscopy images of dried CNF before water reabsorption cycles, 5DC (4a), 25DC (4b), 45DC (4c). After five water reabsorption cycles, 5DC (4d), 25DC (4e), and 45DC (4 f). CNF, cellulose nanofibers; 5DC, 25DC, and 45DC, CNF dried at 5, 25, and 45 °C, respectively.

displayed a more compact structure than the 45DC sample, slightly reducing porosity. These visible distinctions align with previous findings (Andree et al., 2021; Barajas-Ledesma et al., 2020; Klemm et al., 2018) and do not provide a definitive explanation for the structural changes observed in the 25DC sample. Our hypothesis is that the extended air drying time could contribute to the nuanced differences seen in the 25DC sample.

After five reabsorption cycles, significant structural changes in all three dried CNF samples were evident from the SEM images

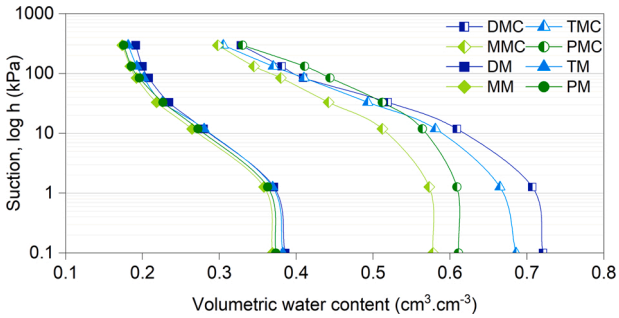

Fig. 5. Soil water retention curve of bare soil and CNF-amended soil. Masa soil mixed with 1% 5DC was saturated with distilled, tap, masa soil–extracted water, and paddy soil–extracted water are referred to as DMC, TMC, MMC, and PMC, respectively. Masa soil saturated with distilled, tap, masa soil–extracted water, and paddy soil–extracted water are referred to as DM, TM, MM, and PM, respectively. CNF, cellulose nanofibers; 5DC, CNF dried at 5 °C.

(Fig. 4d, e, and f). The initial soft and porous state of the 5DC sample gradually weakened its three-dimensional framework each cycle, reducing its ability to withstand the pressure from the absorbed water molecules (El Idrissi et al., 2022; Olad et al., 2020). This led to hornification, fiber aggregation, and a reduced surface area, resulting in lower water reabsorption efficiency. The denser initial configuration of the 25DC sample naturally resulted in a diminished reabsorption capacity.

In summary, analyzing the chemical and morphological structures of CNF elucidates the effects of drying practices and multiple reabsorption cycles on its water absorbency behavior. The findings demonstrate that CNF retains water-holding properties after a series of wet-dry cycles, which mimic basic aspects of natural rainfall and drought patterns. These characteristics suggest that CNF has the potential to be a valuable soil amendment for sustainable land management. However, our evaluation of CNF's water absorption capacity was limited to five cycles due to time constraints, primarily addressing the short-term durability of CNF in soil. Further research could explore the long-term longevity of CNF in soil under various environmental conditions, thus contributing to the development of an effective soil amendment for agricultural practices.

3.2. *Effects of irrigation water quality and CNF addition on the SWRC*

Fig. 5 shows the combined effects of CNF addition and irrigation water quality on the SWRCs for MS and CNF-amended soils. The volumetric water content for the bare MS in the saturated state was 0.37–0.39 $cm^3.cm^{-3}$, which increased to 0.58–0.72 $cm^3.cm^{-3}$, a 156–187% increase after adding 1% CNF.

Significant differences in water retention were determined using two-way ANOVA (Tukey) when examining the effects of water quality on CNF-amended soil. The water retention values of the soil sample irrigated with DW (DMC) and TW (TMC) were higher than those irrigated with MW (MMC) and PW (PMC). This finding highlights the profound influence of CNF amendment and irrigation water quality on water retention, especially at field capacity ($\psi_m > -33$ kPa).

The impact of water quality on the volumetric water content was observed. For the MS sample, the impact of water quality remained consistent across the -1 to -300 kPa range, without significant variations at each suction point ($p > 0.05$). In contrast, the effect of water quality in the CNF-amended soil samples began to diminish within the same pressure range. By the -300 kPa mark, differences attributed to water quality became minimal, highlighting the role of CNF in influencing water retention at this point.

CNF, with its nanoscale fibrous structure in Table A.1, enhances the soil water-holding as shown in Fig. 5. The interactions between CNF and water involve overlapping processes including hydration, condensation, wetting, and diffusion (Solhi et al., 2023). These processes are facilitated by various forces, such as hydrogen bonding, electrostatic interactions, and Van Der Waals forces (Huynh et al., 2023; Reid et al., 2017; Solhi et al., 2023). The isotropic network of CNF contributes to increased water absorption (Solhi et al., 2023). Specifically, the CNF network swelling increases a larger surface area and the number of available hydroxyl groups (Huynh et al., 2023; Solhi et al., 2023), which are primary sites for water interaction on the CNF-soil surface, influencing its absorption rate and volume. Consequently, introducing CNF into soil creates additional absorption sites, enhancing the soil water retention ability.

Apart from CNF, the quality of irrigation water such as ionic profile and pH levels significantly affected soil hydration dynamics (Table A.3). Concentration and composition of ions can alter the balance between surface and cation hydration, affecting water uptake and release in CNF-amended soil (Banedjschafie and Durner, 2015; Barajas-Ledesma et al., 2021; Rattan et al., 2022). Native CNF, which typically have a low negative surface charge (Li et al., 2021), encounter ions in irrigation water that cause thinning of the electrical double layer surrounding the fibrils, thus encouraging fibril aggregation (Huynh et al., 2023). This results in smaller interfibrillar distances and larger contact points, diminishing the trapped water molecules between the fibrils (Arola et al., 2022). Therefore, ions in irrigation water significantly reduce the inherently high water absorption of CNF, emphasizing the complex factors affecting water absorption in nanocellulose networks.

Regarding water pH, CNF is most effective in retaining water at a neutral pH (around 7) (Mahfoudhi and Boufi, 2016). In the examined water samples with pH 5.7–7.3, subtle shifts in CNF-water molecule interaction possibly affected the SWRC. However, even at near-neutral pH, the higher cation concentrations in MW resulted in less water retention of CNF-amended soil than PW (Table A.3). This suggests the ion concentration and composition in irrigation water might be more influential than pH. Further research is required

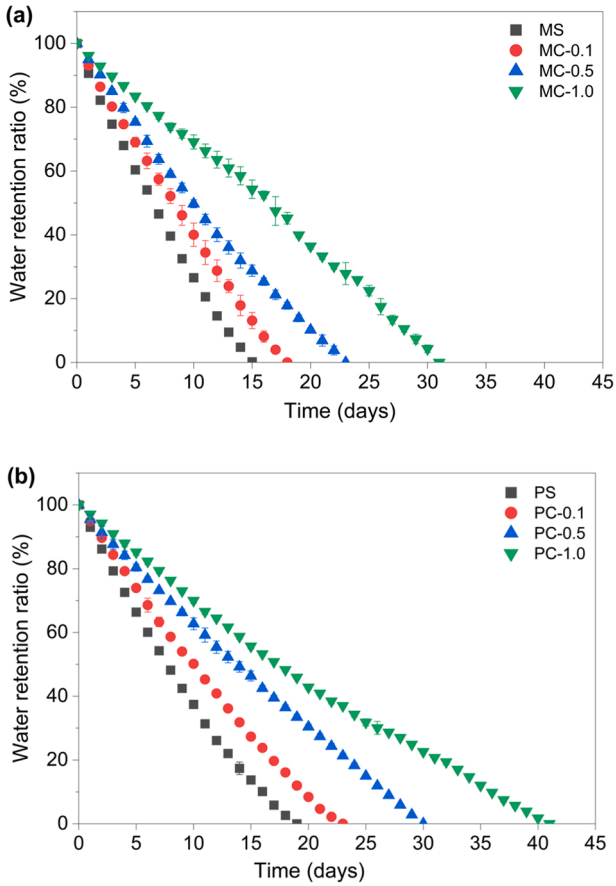

Fig. 6. Water retention ratio of CNF-amended masa soil (6a) and paddy soil (6b). Masa soil mixed with 0.1%, 0.5%, and 1% CNF are referred to as MC-0.1, MC-0.5, and MC-1.0. Paddy soil with similar dosages are referred to as PC-0.1, PC-0.5, and PC-1.0, respectively. CNF, cellulose nanofiber; MS, masa soil; PS, paddy soil.

to clarify the combined effects of pH and ion levels on CNF-soil hydration.

Refining the use of CNF in soil management and optimizing irrigation strategies is crucial. Understanding the interactions between CNF and water qualities and manipulating the ion concentration and pH of irrigation water can maximize the water retention of CNF-amended soils and reduce irrigation frequency. This approach highlights the potential of CNF in advancing sustainable agricultural practice and water management.

3.3. Effect of soil types and CNF dosages on soil water retention time

Fig. 6 shows the marked improvements in the water retention capacity of the CNF-amended soils compared with their non-amended counterparts. The water retention time of PS was longer than that of MS. Fig. 6a illustrates the upward trend in water retention time with increasing CNF dosage in the MS samples. Specifically, the non-CNF-amended MS samples released all absorbed water within 15 days, whereas the CNF-amended MS samples retained moisture for up to 31 days. The incremental CNF dosages of 0.1%, 0.5%, and 1.0% extended water retention duration by 3, 8, and 16 days, respectively.

Similarly, the non-CNF-amended PS samples lost moisture after 19 days (Fig. 6b), while the CNF-amended PS samples retained water for 41 days. The CNF-amended PS samples with 0.1%, 0.5%, and 1.0% CNF retained water for an additional 4, 11, and 22 days, respectively, highlighting remarkable influence of CNF on PS water retention time.

Barajas-Ledesma et al. (2022) demonstrated the beneficial effect of CNF application on soil water retention time; however, they did not explore the influence of different soil characteristics. Our findings indicate that the ability of soil water retention is influenced by its texture and presence of CNF.

Water retention in soil is influenced by a combination of its chemical composition and physical structure. While adsorptive forces related to the soil type play a crucial role, capillary action within pore spaces, dependent on soil particle size and pore dimensions, primarily governs water retention physically (Saha et al., 2020; Zhou et al., 2020). Consequently, sandy soils, with larger particles and wider pores, generally exhibit a lower water retention capacity than silt loam soils. Consistent with this understanding, our results demonstrated that the bare PS sample had better water retention than the bare MS sample.

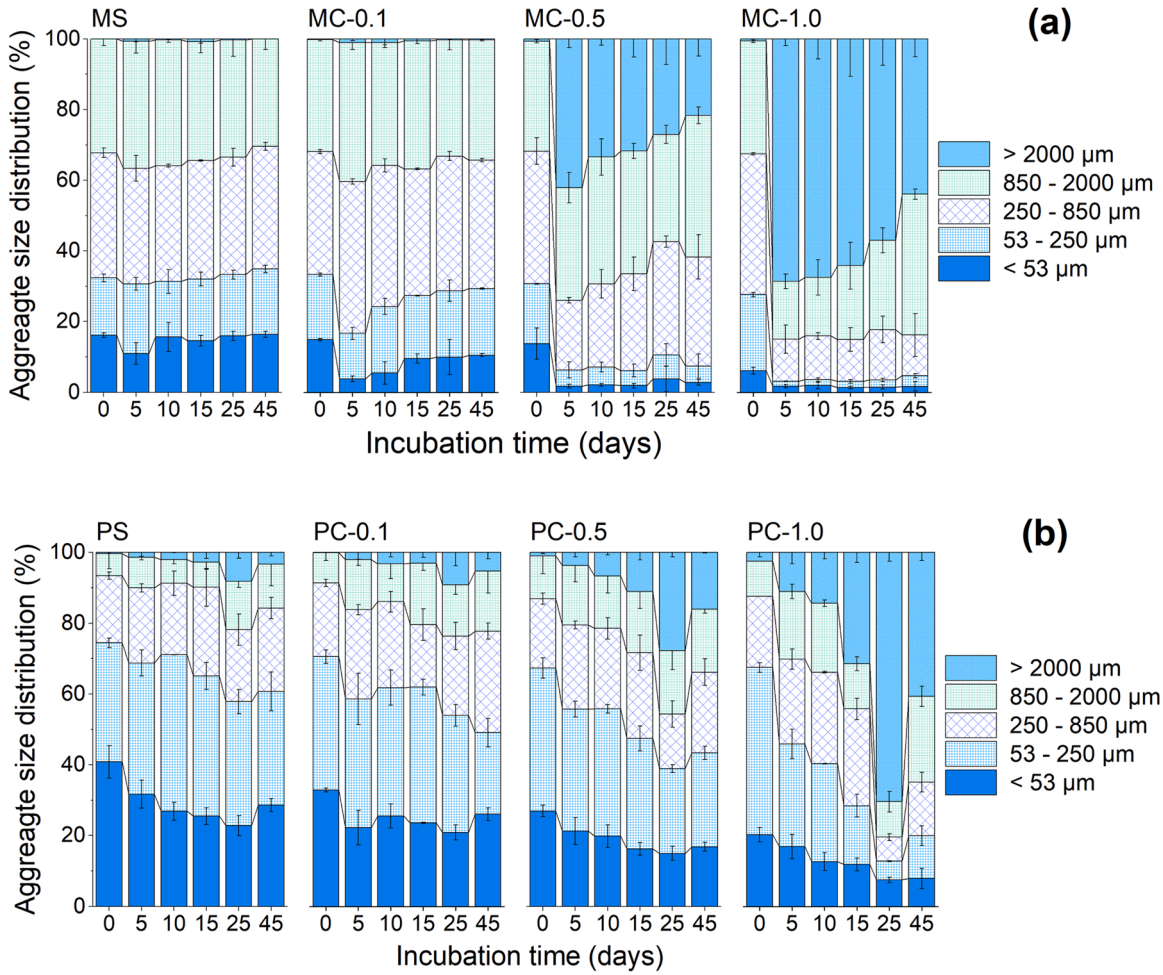

Fig. 7. Aggregate size distribution of CNF-amended masa soil (7a) and paddy soil (7b). Masa soil mixed with 0.1%, 0.5%, and 1% CNF are referred to as MC-0.1, MC-0.5, and MC-1.0. Paddy soil with similar dosages are referred to as PC-0.1, PC-0.5, and PC-1.0, respectively. CNF, cellulose nanofiber; MS, masa soil; PS, paddy soil.

Since the addition of CNF, the water absorbed by the CNF structure along with the CNF fibers themselves occupy the soil pores (Bian et al., 2018; Rahmati et al., 2019). As the CNF application rate increases, the amount of water that retained in the natural soil pores decreases. However, this decrease is offset by the high water storage capability of the three-dimensional network of CNF, which is more efficient than the capillary pores in bare soil.

Additionally, observations from Dorraji et al. (2010); Saha et al. (2020), which involved soil amendments similar to CNF, have demonstrated interactions with smaller soil particles leading to an increase in the specific surface area, a crucial factor for enhancing water retention. These interactions are notably more pronounced in fine-textured soils. Such evidence supports our findings that the application of CNF can more effectively prolong water retention time in PS compared to MS.

Interestingly, preliminary observations from the water retention time experiments hinted at an enhanced interaction among finer soil particles, potentially facilitating the formation of soil aggregates. The subsequent section provides a detailed examination of how CNF contributes to the promotion of these soil aggregates.

3.4. Effect of soil types and CNF dosages on SA size distribution and stability

3.4.1. SA size distribution

Before CNF application, meso-aggregates (250–850 µm) were predominant in the MS samples, whereas nano-aggregates (< 53 µm) were abundant in the PS samples (Fig. 7). By Day 5, minor alterations without significant macroaggregate formation occurred in the bare MS samples. Conversely, changes in the bare PS samples became apparent by Day 25, with macro-aggregates (> 850 µm) making up to 8% of the total aggregates.

CNF introduction facilitated macro-aggregates formation and reduced nano-aggregates in both soil types. Compared with the control, the macro-aggregates in the MS samples treated with 1.0% CNF increased by 48% by Day 5 (Fig. 7a). The largest macro-

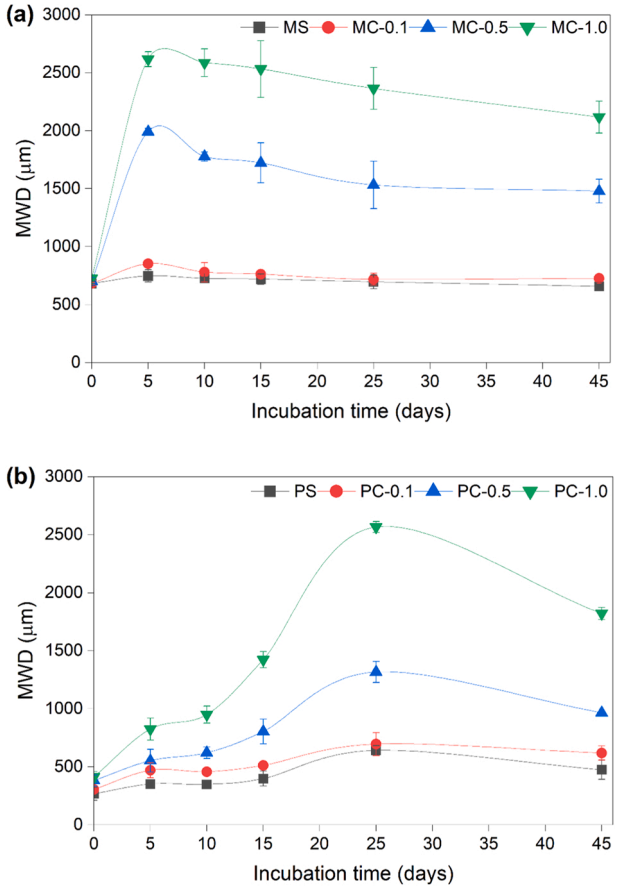

Fig. 8. Mean weight diameter of CNF-amended masa soil (8a) and paddy soil (8b). Masa soil mixed with 0.1%, 0.5%, and 1% CNF are referred to as MC-0.1, MC-0.5, and MC-1.0. Paddy soil with similar dosages are referred to as PC-0.1, PC-0.5, and PC-1.0, respectively. CNF, cellulose nanofiber; MS, masa soil; PS, paddy soil.

aggregates in the CNF-amended PS samples (> 2000 μm) increased from 8% to 70% by Day 25, with total macro-aggregate sizes (> 850 μm) growing by 59% (Fig. 7b).

Recent research by Okebalama & Marschner (2023); Situ et al. (2022) highlights the role of soil amendments similar to CNF (e.g., starch and cellulose), which act as nutrient sources and stimulate microbial activity, thereby enhancing soil-binding forces and promoting aggregate stability. In alignment with these findings, the increase in aggregates observed in our study may be attributed to the soil organic carbon derived from CNF. Additionally, Mizuta et al. (2015) hypothesized that the physical adhesive properties of cellulose with soil water contribute to aggregate formation. In our study, the use of CNF—nanoscale cellulose fibers—may provide more water contact area compared to regular-sized cellulose, potentially enhancing this adhesive effect and supporting the hypothesis. Specifically, CNF augments colloid flocculation and adhesion to soil particle surfaces after water absorption, strengthening chemical bonds in aggregate formation (Shao et al., 2023a; Situ et al., 2022). However, the dynamics of CNF and microbial populations in various soils require further research to elucidate their complex interactions.

3.4.2. SA stability

MWD served as the primary indicator of aggregate stability. The MWD of the MS samples reached peaked on Day 5, while that of the PS samples peaked on Day 25 (Fig. 8). This finding highlights the positive effects of CNF on SA formation in different soil types. For example, SOM facilitates cohesion among soil particles, leading to larger and more resilient aggregates (Mizuta et al., 2015; Okebalama and Marschner, 2023; Situ et al., 2022). Hence, the organic polymer nature and nanoscale characteristics of CNF render its ability to stabilize SA.

The fast rise of stability for MC and slow rise for PC might be related to the inorganic and organic process of the aggregation, since biological process usually takes time. Actually, MC shows lower OM while PC shows higher OM (Table A.2).

The MWD of the soil samples exhibited a slight decrease after reaching their peak, yet SA stability was notably maintained. For instance, improved SA stability persisted for 40 days in the MS samples and 20 days in the PS samples following their peak MWD. Previous studies (Mizuta et al., 2015; Sarker et al., 2018) reported similar trends of sustained SA stability beyond peak MWD, though the underlying mechanisms behind SA stability remain unknown. Various hypotheses have pointed to the critical roles of biochemical

factors, as well as soil nutrients and pH, in influencing microbial activities and root behaviors, thereby impacting SA structures (Abiven et al., 2009; Kang et al., 2022; Situ et al., 2022). While further study is essential to elucidate the complex relationship between physicochemical transformations, microbial dynamics, and SA stability, our findings indicate that CNF has the potential to positively affect SA formation rates and contribute to stability maintenance.

4. Conclusions

In conclusion, this study delves into the multifaceted roles of CNF in soil management, showcasing its effectiveness as a water-saving and soil-stabilizing agent. CNF significantly improves soil water retention and aggregate stability, positively contributing to soil health. The interplay of CNF addition, soil properties, and irrigation water quality showed that CNF promoted soil water conservation and aggregate formation, offering potential benefits to soil management practices.

Our study lays a solid foundation, emphasizing the immediate benefits of CNF while highlighting the need for further exploration of its long-term impacts. Critical areas such as soil microbial properties, nutrient conservation, and the durability of CNF under real-world conditions require in-depth investigation to evaluate the sustainability of CNFs in soil management.

CNF is a promising avenue for promoting environmentally sustainable agriculture. Optimization of CNF application methods can profoundly impact soil management strategies, contributing to a more sustainable approach to agriculture and enhancing food security.

CRediT authorship contribution statement

Long Thanh Bui: Writing – review & editing, Methodology. **An Thuy NGO:** Writing – original draft, Methodology, Investigation, Conceptualization. **Yasushi Mori:** Writing – review & editing, Supervision, Resources, Methodology, Funding acquisition, Conceptualization.

Declaration of Competing Interest

The authors declare that they have no competing interests.

Data availability

Data will be made available on request.

Acknowledgments

The authors are grateful to Dr. Jun Kano at Graduate School of Environmental, Life, Natural Science and Technology, Okayama University for his advice on FTIR and SEM measurements. This study was partially supported by the Japan Society for the Promotion of Science NEXT Program (GS021, 2011–2014), KAKENHI (B) (26292127, 2014–2016), KAKENHI (A) (17H01496, 2017–2020), (21H04747, 2021–2024) and KAKENHI (S) (24H00057, 2024–2028). This research was conducted as part of the ABRESO project and supported by the Japan Science and Technology Agency as part of the Belmont Forum.

Appendix A. Supporting information

Supplementary data associated with this article can be found in the online version at doi:10.1016/j.eti.2024.103650.

References

Abiven, S., Menasseri, S., Chenu, C., 2009. The effects of organic inputs over time on soil aggregate stability–a literature analysis. Soil Biol. Biochem. 41, 1–12. https://doi.org/10.1016/J.SOILBIO.2008.09.015.

Alsulaili, A., Alkandari, M., Buqammaz, A., 2022. Assessing the impacts of meteorological factors on freshwater consumption in arid regions and forecasting the freshwater demand. Environ. Technol. Innov. 25, 102099 https://doi.org/10.1016/J.ETI.2021.102099.

Andree, V., Niopek, D., Müller, C., Eiselt, J.-P., Foh, N., Rzany, A., Hensel, B., 2021. Influence of drying methods on the physical properties of bacterial nanocellulose. Mater. Res. Express 8, 025402. https://doi.org/10.1088/2053-1591/abe016.

Arola, S., Kou, Z., Rooijakkers, B.J.M., Velagapudi, R., Sammalkorpi, M., Linder, M.B., 2022. On the mechanism for the highly sensitive response of cellulose nanofiber hydrogels to the presence of ionic solutes. Cellulose 29, 6109–6121. https://doi.org/10.1007/s10570-022-04664-w.

Banedjschafie, S., Durner, W., 2015. Water retention properties of a sandy soil with superabsorbent polymers as affected by aging and water quality. J. Plant Nutr. Soil Sci. 178, 798–806. https://doi.org/10.1002/jpln.201500128.

Barajas-Ledesma, R.M., Hossain, L., Wong, V.N.L., Patti, A.F., Garnier, G., 2021. Effect of the counter-ion on nanocellulose hydrogels and their superabsorbent structure and properties. J. Colloid Interface Sci. 599, 140–148. https://doi.org/10.1016/J.JCIS.2021.04.065.

Barajas-Ledesma, R.M., Patti, A.F., Wong, V.N.L., Raghuwanshi, V.S., Garnier, G., 2020. Engineering nanocellulose superabsorbent structure by controlling the drying rate. Colloids Surf. A Physicochem. Eng. Asp. 600, 124943 https://doi.org/10.1016/J.COLSURFA.2020.124943.

Barajas-Ledesma, R.M., Wong, V.N.L., Little, K., Patti, A.F., Garnier, G., 2022. Carboxylated nanocellulose superabsorbent: biodegradation and soil water retention properties. J. Appl. Polym. Sci. 139 https://doi.org/10.1002/app.51495.

Bauli, C.R., Lima, G.F., de Souza, A.G., Ferreira, R.R., Rosa, D.S., 2021. Eco-friendly carboxymethyl cellulose hydrogels filled with nanocellulose or nanoclays for agriculture applications as soil conditioning and nutrient carrier and their impact on cucumber growing. Colloids Surf. A Physicochem. Eng. Asp. 623, 126771 https://doi.org/10.1016/j.colsurfa.2021.126771.

Bhattacharyya, R., Rabbi, S.M.F., Zhang, Y., Young, I.M., Jones, A.R., Dennis, P.G., Menzies, N.W., Kopittke, P.M., Dalal, R.C., 2021. Soil organic carbon is significantly associated with the pore geometry, microbial diversity and enzyme activity of the macro-aggregates under different land uses. Sci. Total Environ. 778, 146286 https://doi.org/10.1016/J.SCITOTENV.2021.146286.

Bian, X., Zeng, L., Deng, Y., Li, X., 2018. The role of superabsorbent polymer on strength and microstructure development in cemented dredged clay with high water content. Polymers 10. https://doi.org/10.3390/polym10101069.

Bui, L.T., Mori, Y., 2021. Pinhole multistep centrifuge outflow method for estimating unsaturated hydraulic properties with small volume soil samples. Water 13. https://doi.org/10.3390/w13091169.

Bui, T.L., Mori, Y., Maeda, M., Somura, H., 2022. Artificial macropores and water management effects on reduction of greenhouse gas emissions from rice paddy fields. Environ. Chall. 9, 100657 https://doi.org/10.1016/j.envc.2022.100657.

Campbell, G.S., Campbell, C.S., 2013. Water content and potential, measurement. Ref. Modul. Earth Syst. Environ. Sci. https://doi.org/10.1016/B978-0-12-409548-9.05333-1.

Chang, C., He, M., Zhou, J., Zhang, L., 2011. Swelling behaviors of pH- and salt-responsive cellulose-based hydrogels. Macromolecules 44, 1642–1648. https://doi.org/10.1021/ma102801f.

Chavez-Rico, V.S., van den Bergh, S., Bodelier, P.L.E., van Eekert, M., Luo, Y., Nierop, K.G.J., Sechi, V., Veeken, A., Buisman, C., 2023. Effect of pre-treatment processes of organic residues on soil aggregates. Environ. Technol. Innov. 30, 103104 https://doi.org/10.1016/J.ETI.2023.103104.

Chen, L., Sun, S., Zhou, Y., Zhang, B., Peng, Y., Zhuo, Y., Ai, W., Gao, C., Wu, B., Liu, D., Sun, C., 2023. Straw and straw biochar differently affect fractions of soil organic carbon and microorganisms in farmland soil under different water regimes. Environ. Technol. Innov. 32, 103412 https://doi.org/10.1016/J.ETI.2023.103412.

Coates, J., 2006. Interpretation of infrared spectra (https://doi.org/https. https://doi.org/). A Pract. Approach Encycl. Anal. Chem.. https://doi.org/10.1002/9780470027318.a5606.

Dane, J.H., Topp, G.C., Campbell, G.S., Horton, R., Jury, W.A., Nielsen, D.R., Es, H.M., Amoodi, L.A., Dick, W.A., 2002. Methods of soil analysis. Part 4. Physical methods. Soil Sci. Soc. Am. https://doi.org/10.2113/3.2.722.

Dexter, A.R., 2004. Soil physical quality: part I. Geoderma 120, 201–214. https://doi.org/10.1016/j.geoderma.2003.09.004.

Dhiman, J., Prasher, S.O., ElSayed, E., Patel, R.M., Nzediegwu, C., Mawof, A., 2021. Effect of hydrogel based soil amendments on yield and growth of wastewater irrigated potato and spinach grown in a sandy soil. Environ. Technol. Innov. 23, 101730 https://doi.org/10.1016/J.ETI.2021.101730.

Djafari Petroudy, S.R.D., Ranjbar, J., Rasooly Garmaroody, E., 2018. Eco-friendly superabsorbent polymers based on carboxymethyl cellulose strengthened by TEMPO-mediated oxidation wheat straw cellulose nanofiber. Carbohydr. Polym. 197, 565–575. https://doi.org/10.1016/J.CARBPOL.2018.06.008.

Dorraji, S.S., Golchin, A., Ahmadi, S., 2010. The effects of hydrophilic polymer and soil salinity on corn growth in sandy and loamy soils. CLEAN Soil Air Water 38, 584–591. https://doi.org/10.1002/clen.201000017.

Elliott, E.T., 1986. Aggregate structure and carbon, nitrogen, and phosphorus in native and cultivated soils. Soil Sci. Soc. Am. J. 50, 627–633. https://doi.org/10.2136/sssaj1986.03615995005000030017x.

Gharib, A.A., Blumberg, J., Manning, D.T., Goemans, C., Arabi, M., 2023. Assessment of vulnerability to water shortage in semi-arid river basins: the value of demand reduction and storage capacity. Sci. Total Environ. 871, 161964 https://doi.org/10.1016/J.SCITOTENV.2023.161964.

Gill, S.J., Wadsö, I., 1976. An equation of state describing hydrophobic interactions (https://www.pnas.org.). Proc. Natl. Acad. Sci. Usa. 73, 2955–2958. https://doi.org/10.1073/pnas.73.9.2955.

Huynh, N., Valle-Delgado, J.J., Fang, W., Arola, S., Österberg, M., 2023. Tuning the water interactions of cellulose nanofibril hydrogels using willow bark extract. Carbohydr. Polym. 317, 121095 https://doi.org/10.1016/j.carbpol.2023.121095.

Ide, J., Takeda, I., Somura, H., Mori, Y., Sakuno, Y., Yone, Y., Takahashi, E., 2019. Impacts of hydrological changes on nutrient transport from diffuse sources in a rural river basin, Western Japan. J. Geophys. Res. Biogeosci. 124, 2565–2581. https://doi.org/10.1029/2018JG004513.

El Idrissi, A., El Gharrak, A., Achagri, G., Essamlali, Y., Amadine, O., Akil, A., Sair, S., Zahouily, M., 2022. Synthesis of urea-containing sodium alginate-g-poly (acrylic acid-co-acrylamide) superabsorbent-fertilizer hydrogel reinforced with carboxylated cellulose nanocrystals for efficient water and nitrogen utilization. J. Environ. Chem. Eng. 10 https://doi.org/10.1016/j.jece.2022.108282.

Jat, M.L., Gathala, M.K., Choudhary, M., Sharma, S., Jat, H.S., Gupta, N., Yadvinder-Singh, 2023. Conservation agriculture for regenerating soil health and climate change mitigation in smallholder systems of South Asia. Adv. Agron. 181, 183–277. https://doi.org/10.1016/BS.AGRON.2023.05.003.

Kaffashsaie, E., Yousefi, H., Nishino, T., Matsumoto, T., Mashkour, M., Madhoushi, M., Kawaguchi, H., 2021. Direct conversion of raw wood to TEMPO-oxidized cellulose nanofibers. Carbohydr. Polym. 262, 117938 https://doi.org/10.1016/J.CARBPOL.2021.117938.

Kang, M.W., Yibeltal, M., Kim, Y.H., Oh, S.J., Lee, J.C., Kwon, E.E., Lee, S.S., 2022. Enhancement of soil physical properties and soil water retention with biochar-based soil amendments. Sci. Total Environ. 836, 155746 https://doi.org/10.1016/j.scitotenv.2022.155746.

Klemm, D., Cranston, E.D., Fischer, D., Gama, M., Kedzior, S.A., Kralisch, D., Kramer, F., Kondo, T., Lindström, T., Nietzsche, S., Petzold-Welcke, K., Rauchfuß, F., 2018. Nanocellulose as a natural source for groundbreaking applications in materials science: Today's state. Mater. Today 21, 720–748. https://doi.org/10.1016/J.MATTOD.2018.02.001.

Liu, J., Li, Q., Su, Y., Yue, Q., Gao, B., 2014. Characterization and swelling–deswelling properties of wheat straw cellulose based semi-IPNs hydrogel. Carbohydr. Polym. 107, 232–240. https://doi.org/10.1016/J.CARBPOL.2014.02.073.

Li, M.C., Wu, Q., Moon, R.J., Hubbe, M.A., Bortner, M.J., 2021. Rheological aspects of cellulose nanomaterials: governing factors and emerging applications. Adv. Mater. 33, e2006052 https://doi.org/10.1002/adma.202006052.

Mahfoudhi, N., Boufi, S., 2016. Poly (acrylic acid-co-acrylamide)/cellulose nanofibrils nanocomposite hydrogels: effects of CNFs content on the hydrogel properties. Cellulose 23, 3691–3701. https://doi.org/10.1007/s10570-016-1074-z.

Marczak, D., Lejcuś, K., Kulczycki, G., Misiewicz, J., 2022. Towards circular economy: sustainable soil additives from natural waste fibres to improve water retention and soil fertility. Sci. Total Environ. 844, 157169 https://doi.org/10.1016/J.SCITOTENV.2022.157169.

Mizuta, K., Taguchi, S., Sato, S., 2015. Soil aggregate formation and stability induced by starch and cellulose. Soil Biol. Biochem. 87, 90–96. https://doi.org/10.1016/J.SOILBIO.2015.04.011.

Morioka, E., Bui, T.L., Mori, Y., Osawa, K., Hoshikawa, A., 2023. Linear macropore installation to reduce red-soil erosion in sugarcane fields. J. Soil Sci. Plant Nutr. 23, 4572–4582. https://doi.org/10.1007/s42729-023-01373-6.

Mori, Y., Fujihara, A., Yamagishi, K., 2014. Installing artificial macropores in degraded soils to enhance vertical infiltration and increase soil carbon content. Prog. Earth Planet. Sci. 1, 30. https://doi.org/10.1186/s40645-014-0030-5.

Mori, Y., Iwama, K., Maruyama, T., Mitsuno, T., 1999. Discriminating the influence of soil texture and management-induced changes in macropore flow using soft X-rays. https://journals.lww.com/soilsci/Fulltext/1999/07000/DISCRIMINATING_THE_INFLUENCE_OF_SOIL_TEXTURE_AND.3.aspx Soil Sci. 164, 467–482. https://doi.org/10.1097/00010694-199907000-00003.

Mori, Y., Suetsugu, A., Matsumoto, Y., Fujihara, A., Suyama, K., 2013. Enhancing bioremediation of oil-contaminated soils by controlling nutrient dispersion using dual characteristics of soil pore structure. Ecol. Eng. 51, 237–243. https://doi.org/10.1016/j.ecoleng.2012.12.009.

Okebalama, C.B., Marschner, B., 2023. Reapplication of biochar, sewage waste water, and NPK fertilizers affects soil fertility, aggregate stability, and carbon and nitrogen in dry-stable aggregates of semi-arid soil. Sci. Total Environ. 866, 161203 https://doi.org/10.1016/J.SCITOTENV.2022.161203.

Olad, A., Doustdar, F., Gharekhani, H., 2020. Fabrication and characterization of a starch-based superabsorbent hydrogel composite reinforced with cellulose nanocrystals from potato peel waste. Colloids Surf. A Physicochem. Eng. Asp. 601, 124962 https://doi.org/10.1016/J.COLSURFA.2020.124962.

Qin, C.-C., Abdalkarim, S.Y.H., Zhou, Y., Yu, H.-Y., He, X., 2022. Ultrahigh water-retention cellulose hydrogels as soil amendments for early seed germination under harsh conditions. J. Clean. Prod. 370, 133602 https://doi.org/10.1016/j.jclepro.2022.133602.

Qi, J.Y., Han, S.W., Lin, B.J., Xiao, X.P., Jensen, J.L., Munkholm, L.J., Zhang, H.L., 2022. Improved soil structural stability under no-tillage is related to increased soil carbon in rice paddies: Evidence from literature review and field experiment. Environ. Technol. Innov. 26, 102248 https://doi.org/10.1016/J.ETI.2021.102248.
Quintana, J.R., Martín-Sanz, J.P., Valverde-Asenjo, I., Molina, J.A., 2023. Drought differently destabilizes soil structure in a chronosequence of abandoned agricultural lands. CATENA 222, 106871. https://doi.org/10.1016/J.CATENA.2022.106871.
Rahmati, M., Pohlmeier, A., Abasiyan, S.M.A., Weihermüller, L., Vereecken, H., 2019. Water retention and pore size distribution of a biopolymeric-amended loam soil. Vadose Zone J. 18, 1–13. https://doi.org/10.2136/vzj2018.11.0205.
Rattan, B., Dhobale, K.V., Saha, A., Garg, A., Sahoo, L., Sreedeep, S., 2022. Influence of inorganic and organic fertilizers on the performance of water-absorbing polymer amended soils from the perspective of sustainable water use efficiency. Soil . Res. 223, 105449 https://doi.org/10.1016/J.STILL.2022.105449.
Reid, M.S., Kedzior, S.A., Villalobos, M., Cranston, E.D., 2017. Effect of ionic strength and surface charge density on the kinetics of cellulose nanocrystal thin film swelling. Langmuir 33, 7403–7411. https://doi.org/10.1021/acs.langmuir.7b01740.
Reshmy, R., Philip, E., Madhavan, A., Arun, K.B., Binod, P., Pugazhendhi, A., Awasthi, M.K., Gnansounou, E., Pandey, A., Sindhu, R., 2021. Promising eco-friendly biomaterials for future biomedicine: cleaner production and applications of nanocellulose. Environ. Technol. Innov. 24, 101855 https://doi.org/10.1016/J.ETI.2021.101855.
Saha, A., Rattan, B., Sekharan, S., Manna, U., 2020. Quantifying the interactive effect of water absorbing polymer (WAP)-soil texture on plant available water content and irrigation frequency. Geoderma 368, 114310. https://doi.org/10.1016/J.GEODERMA.2020.114310.
Sarker, T.C., Incerti, G., Spaccini, R., Piccolo, A., Mazzoleni, S., Bonanomi, G., 2018. Linking organic matter chemistry with soil aggregate stability: Insight from 13C NMR spectroscopy. Soil Biol. Biochem. 117, 175–184. https://doi.org/10.1016/J.SOILBIO.2017.11.011.
Shao, B., Han, Z., Pang, R., Wu, D., Xie, B., Su, Y., 2023b. The crystalline structure transition and hydrogen bonds shift determining enhanced enzymatic digestibility of cellulose treated by ultrasonication. Sci. Total Environ. 876, 162631 https://doi.org/10.1016/j.scitotenv.2023.162631.
Shao, F., Zeng, S., Wang, Q., Tao, W., Wu, J., Su, L., Yan, H., Zhang, Y., Lin, S., 2023a. Synergistic effects of biochar and carboxymethyl cellulose sodium (CMC) applications on improving water retention and aggregate stability in desert soils. J. Environ. Manag. 331, 117305 https://doi.org/10.1016/J.JENVMAN.2023.117305.
Situ, Y., Yang, Y., Huang, C., Liang, S., Mao, X., Chen, X., 2023. Effects of several superabsorbent polymers on soil exchangeable cations and crop growth. Environ. Technol. Innov. 30, 103126 https://doi.org/10.1016/J.ETI.2023.103126.
Situ, G., Zhao, Y., Zhang, L., Yang, X., Chen, D., Li, S., Wu, Q., Xu, Q., Chen, J., Qin, H., 2022. Linking the chemical nature of soil organic carbon and biological binding agent in aggregates to soil aggregate stability following biochar amendment in a rice paddy. Sci. Total Environ. 847, 157460 https://doi.org/10.1016/J.SCITOTENV.2022.157460.
Solhi, L., Guccini, V., Heise, K., Solala, I., Niinivaara, E., Xu, W., Mihhels, K., Kröger, M., Meng, Z., Wohlert, J., Tao, H., Cranston, E.D., Kontturi, E., 2023. Understanding nanocellulose–water interactions: Turning a detriment into an asset. Chem. Rev. 123, 1925–2015. https://doi.org/10.1021/acs.chemrev.2c00611.
Sparks, D.L., Page, A.L., Helmke, P.A., Loeppert, R.H., Soltanpour, P.N., Tabatabai, M.A., Johnston, C.T., Sumner, M.E., 1996. Methods of soil analysis. Part 3 Chemical Methods. Soil Science Society of America, American Society of Agronomy. https://doi.org/10.2136/sssabookser5.3.
Stanisławska, A., Staroszczyk, H., Szkodo, M., 2020. The effect of dehydration/rehydration of bacterial nanocellulose on its tensile strength and physicochemical properties. Carbohydr. Polym. 236, 116023 https://doi.org/10.1016/J.CARBPOL.2020.116023.
Wang, Y., Lian, J., Wan, J., Ma, Y., Zhang, Y., 2015. A supramolecular structure insight for conversion property of cellulose in hot compressed water: polymorphs and hydrogen bonds changes. Carbohydr. Polym. 133, 94–103. https://doi.org/10.1016/j.carbpol.2015.06.110.
Zhang, Z., Abidi, N., Lucia, L., Chabi, S., Denny, C.T., Parajuli, P., Rumi, S.S., 2023. Cellulose/nanocellulose superabsorbent hydrogels as a sustainable platform for materials applications: a mini-review and perspective. Carbohydr. Polym. 299, 120140 https://doi.org/10.1016/j.carbpol.2022.120140.
Zhou, H., Chen, C., Wang, D., Arthur, E., Zhang, Z., Guo, Z., Peng, X., Mooney, S.J., 2020. Effect of long-term organic amendments on the full-range soil water retention characteristics of a vertisol. Soil . Res. 202, 104663 https://doi.org/10.1016/j.still.2020.104663.
Šebenik, U., Lapasin, R., Krajnc, M., 2020. Rheology of aqueous dispersions of laponite and TEMPO-oxidized nanofibrillated cellulose. Carbohydr. Polym. 240, 116330 https://doi.org/10.1016/J.CARBPOL.2020.116330.